
Experimental investigation of damage and fracture in glassy materials at the nanometre scale

D. Bonamy*

Groupe Fracture, DSM/DRECAM/SPCSI, CEA Saclay,
F-91191, Gif sur Yvette Cedex, France
E-mail: bonamy@drecam.cea.fr
*Corresponding author

S. Prades

Groupe Fracture, DSM/DRECAM/SPCSI, CEA Saclay,
F-91191, Gif sur Yvette Cedex, France
Present address: Nanometallurgy, Wolfgang-Pauli-Strasse 10 ETH
Hönggerberg, HCI F 529, CH-8093 Zürich, Switzerland
E-mail: silke.prades@mat.ethz.ch

L. Ponson

Groupe Fracture, DSM/DRECAM/SPCSI, CEA Saclay,
F-91191, Gif sur Yvette Cedex, France
E-mail: ponson@drecam.cea.fr

D. Dalmas

Groupe Fracture, DSM/DRECAM/SPCSI, CEA Saclay,
F-91191, Gif sur Yvette Cedex, France
Present address: Glass Surface & Interface, Unité Mixte
CNRS/Saint-Gobain, F-93303 Aubervilliers Cedex, France
E-mail: Davy.Dalmas@saint-gobain.com

C.L. Rountree, E. Bouchaud and C. Guillot

Groupe Fracture, DSM/DRECAM/SPCSI, CEA Saclay,
F-91191, Gif sur Yvette Cedex, France
E-mail: croutree@cea.fr E-mail: elisabeth.bouchaud@cea.fr
E-mail: cguillot@drecam.cea.fr

Abstract: Slow crack advance is observed in real time via an Atomic Force Microscope in a minimal glass, amorphous Silica, under stress corrosion. Fracture proceeds through the nucleation, growth and coalescence of damage cavities, as recently reported in an aluminosilicate glass. The crack growth velocity as observed at the continuum scale is shown to be dominated by accelerating phases corresponding to the cavity coalescence with the main crack front. The process zone at the crack tip is then determined, and shown to increase with time when both the average crack growth velocity and the

mechanical stress are kept constant. Transport of water molecules within the process zone is conjectured to be the dominant mechanism responsible for this time evolution. Migration of alkali Na ions in more complex Silicate glass is finally evidenced at the sub-micrometric scale by observing through AFM the crack propagation in binary $\text{Na}_2\text{O}/\text{SiO}_2$ glasses.

Keywords: AFM; brittleness; corrosion; fatigue; fracture and cracks.

Reference to this paper should be made as follows: Bonamy, D., Prades, S., Ponson, L., Dalmas, D., Rountree, C.L., Bouchaud, E. and Guillot, C. (2006) 'Experimental investigation of damage and fracture in glassy materials at the nanometre scale', *Int. J. Materials & Product Technology*, Vol. 26, Nos. 3/4, pp.339–353.

Biographical notes: Dr. Daniel Bonamy is a researcher at the Service of Physics and Chemistry of Surfaces and Interfaces (SPCSI) at the French Department of Energy (CEA) in Saclay. He obtained his PhD in Physics in 2001. He is especially interested in understanding the relationships between the microscopic and the continuum scale in granular systems and fracture problems. His principal fields of expertise are statistical physics, experimental methods used in fracture mechanics and near field microscopy.

Dr. Silke Prades obtained a PhD at the SPCSI at CEA in Saclay. She is now a postdoctoral researcher at the Nanometallurgy group of the Department of Materials of the Swiss Federal Institute of Technology (ETH) in Zurich. Her main field of interest is understanding the mechanical properties of materials at their microstructural scale.

Laurent Ponson is currently a PhD student at the SPCSI at CEA in Saclay. He is especially interested in granular systems and fracture problems. He is currently working on physical aspect of fracture, and more precisely on quantitative fractography and 3D effects in fracture mechanics.

Dr. Davy Dalmas is a CNRS researcher at the joint laboratory CNRS/Saint-Gobain Surface of Glass and Interfaces. He obtained his PhD in mechanical sciences in 2001 from Compigne University of Technology (UTC) in France and had a post-doctoral position at the SPCSI at CEA in Saclay in 2002 and 2003. He is currently working on adhesion and scratch resistance of thin film and on morphology and fracture of borosilicate glasses. His principal fields of interest are fracture and damage of heterogeneous materials, acoustic emission and near field microscopy.

Dr. Cindy L. Rountree has an NSF postdoctoral position at the SPCSI at CEA in Saclay. She obtained a Master in Computing Science and a PhD in Physics from Louisiana State University in 2003. Her main field of expertise is molecular dynamics simulations of fracture in silica glasses. She is currently working on a unified study of crack propagation in amorphous silica: using experiments and simulations; plasticity in glasses due to stress-induced nanometre scale structural rearrangements; and atomic force microscopy experiments on stress-corrosion fracture in glasses and algorithm design for the analysis of mechanical damage in these experiments.

Dr. E. Bouchaud is currently Director of the SPCSI at CEA in Saclay. She is on the Advisory Board of Priority 3 (Nanoscience, Materials & Processes) for the 6th European Framework Programme, on the Executive Committee of the International Conference on Fracture, and she is a Regional Editor of the International Journal of Fracture. She is currently working on stress corrosion of glasses. Her main field of interest is fracture and damage of heterogeneous materials, and quantitative fractography.

Dr. Claude Guillot is a researcher at the SPCSI at CEA in Saclay. He obtained a first PhD in Physics, in 1972 from Orsay University in France, and a State PhD with Habilitation to lead research in 1985 from Paris VI University. He has been in charge of the CEA surface physics group on synchrotron radiation from 1990 to 1998. Since 2000 he has been in charge of the 'fracture group' in the Division of Physics and Chemistry of Surfaces and Interfaces. His main scientific topic concerns the fracture of heterogeneous materials.

1 Introduction

Fabrication of materials, structure and devices can currently be controlled at the nanoscale. However, ensuring their strength and their life expectancy over the long term still presents a major challenge. Over the past century, the understanding of material failure has greatly improved and a coherent theoretical framework, the Linear Elastic Fracture Mechanics (LEFM) has developed. This theory states that crack initiation occurs when the mechanical energy G released by crack advance is sufficient to balance the one needed to create new surfaces (Griffith, 1920). In an elastic medium, G is entirely dissipated within a small zone – referred to as *the process zone* located at the crack tip.

Linear Elasticity predicts that the stress field is dominated by a square root singularity in the vicinity of the crack tip (Irwin, 1958; Orowan, 1955). By making use of the universal nature of the near-tip stress field, LEFM relates G to the prefactor of the stress field singularity – referred to as the stress intensity factor K_I – that can be determined in any geometry (Irwin, 1958; Orowan, 1955). However, the way the crack dissipates this flux G by propagating within the process zone is far more problematic. This involves processes occurring at the micro-structure scale of the material, i.e. at a scale out of the range of LEFM. As a matter of fact, classical theories take these phenomena into account through constitutive phenomenological laws and distinguish brittle from ductile fracture.

- For brittle fracture (cleavage of metals or glass breaking for example), it is often thought that the crack progresses by successive breakings of atomic bonds, and does not involve any damage occurring ahead of the crack tip (Kelly et al., 1967; Lawn et al., 1980).
- For ductile fracture (most commonly breaking mode of metallic alloys), the crack advances through the nucleation, growth and coalescence of damage cavities (see for instance Pineau et al. (1995)). In these cases, nucleation usually occurs at microstructural 'defects', such as second phase precipitates unable to accommodate plastic deformation. Then, the voids grow under the action of the stress triaxiality (Rice and Tracey, 1969), and blunt when extending into the metallic matrix.

Description of the failure mechanisms within the process zone is out of the reach of LEFM. Crack surface roughness e.g. involves the material structure at small time and length scale. However, while resulting from material specific processes, the morphology of fracture surfaces exhibits some universal scaling features in a wide range of materials (glasses, metallic alloys, ceramics, woods, rocks, etc.), with various

failure modes (dynamic fracture, stress corrosion, fatigue, etc.) (Bouchaud, 1997). This strongly suggests the existence of some underlying generic mechanisms within the process zone independent both of the precise nature of the material and of the mechanical conditions.

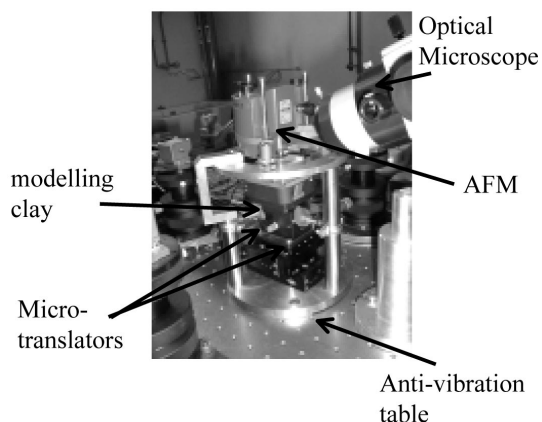
These various results have led us to investigate how crack propagates in a nominally brittle elastic material, silicate glass, at its micro-structure scale through Atomic Force Microscopy (AFM). The first series of experiments, were performed on aluminosilicate glasses with C. Marlière, F. Célarié and their collaborators (Célarié et al., 2003a,b; Marlière et al., 2003). They allowed us to evidence the existence of damage nanoscale cavities growing ahead of the crack tip similar to the one commonly observed during ductile fracture of metallic alloys, but on a scale three orders of magnitude smaller.

A second series of experiments performed on pure amorphous silica was reported in Prades (2004) and Prades et al. (2005). This investigation is extended in this paper. The experimental setup is presented in Section 2. Sections 3 and 4 are devoted to the crack propagation mode as observed within the process zone. Nanoscale damage cavities are evidenced and their kinematic is investigated. Section 5 focuses more precisely on the process zone size and its time evolution. Role of alkalis migrations in more complex binary $\text{Na}_2\text{O}/\text{SiO}_2$ glasses is investigated in Section 6. Finally Section 7 summarises the observations and discusses them.

2 Experimental setup

Observing the failure mechanisms in silica glass at its micro-structure scale requires nanometric spatial resolution. Therefore, Atomic Force Microscopy (AFM) appears to be the most appropriate tool to probe the process zone with good enough spatial resolution. The main drawback actually resides in the recording time of an AFM frame around few minutes. This has led us to work in the ultra slow stress corrosion regime where the time scale of crack propagation is small compared with the recording time of our apparatus. The experimental setup is shown in Figure 1 and briefly described below.

Figure 1 Experimental setup



Fracture is performed on a Double Cleavage Drilled Compression (DCDC) specimen: a parallelepipedic $5 \times 5 \times 25 \text{ mm}^3$ sample of pure silica glass with a hole of radius a drilled in the centre is placed between the jaws of a compressive Deben machine (Figure 2). The pressure σ is then gradually increased up to the initiation of two cracks that propagate symmetrically on both sides of the hole (Figure 2). The reference frame $\vec{e}_x, \vec{e}_y, \vec{e}_z$ is defined so that \vec{e}_x and \vec{e}_z are parallel to the direction of crack propagation and the crack front (or hole axis) respectively (Figure 2).

Figure 2 Double cleavage drilled compression (DCDC) configuration used to fracture the glass sample under stress corrosion

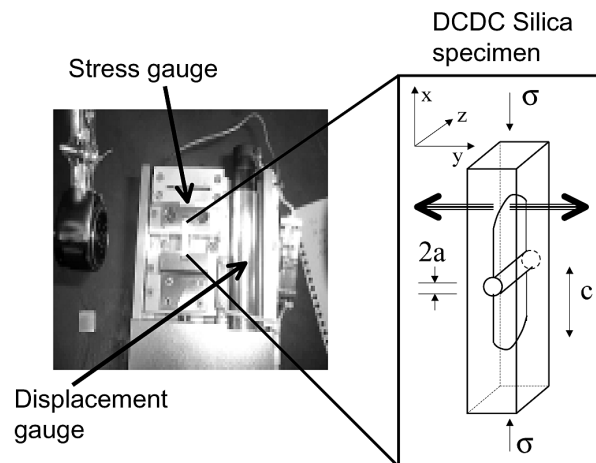
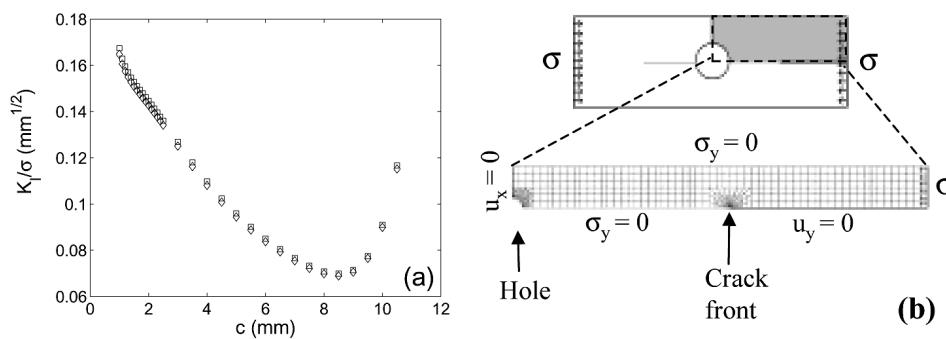


Figure 3 (a) Variation of the geometrical part of the stress intensity factor, K_I/σ , as a function of the crack length c as determined through Finite Element calculation. The diamonds and squares correspond to calculations using the J-integral method and the CTOD method respectively. (b) Diagram of the mesh used in the finite element calculations



In this DCDC geometry, the variation of the geometrical part of the stress intensity factor K_I/σ as a function of the crack length c has been computed by a 2D plane stress analysis through the finite element code CAST3M. The mesh geometry of the simulation is shown in Figure 3(b). Thanks to the symmetry of the geometry, only

one quarter of the specimen – composed of 15306 nodes – was modelled. The Poisson ratio and the Young modulus were set to 0.3 and 70 GPa respectively. Once the stress, strain and displacement field is calculated for the mesh, K_I is evaluated using both J-integral method (Rice, 1968) and Crack Tip Opening Displacement (CTOD) method (Ewalds and Wanhill, 1985). Variation of K_I as a function of c as estimated through these two methods is represented in Figure 3(a).

Let us note that the stress intensity factor K_I decreases when the crack length c increases. The crack growth is then slowing down until K_I decreases under K_{IC} . The crack would then completely stop under vacuum, but in a humid environment, the corrosive action of water on glass allows a slow, sub-critical crack propagation. All our experiments were performed in the room atmosphere during a period while relative humidity and temperature were $45 \pm 3\%$ and $26.0 \pm 2^\circ\text{C}$ respectively. Figure 4 presents the variation of the mean crack tip velocity v as a function of the stress intensity factor K_I in this stress corrosion regime. The exponential behaviour is compatible with stress enhanced activated process models (Célarié et al., 2003b; Wiederhorn, 1967; Wiederhorn and Bolz, 1970).

$$v = v_0 \exp(K_I^2/K_0^2) \quad (1)$$

where v_0 and K_0 are found to be $v_0 \simeq 6.7 \times 10^{-17} \text{ m.s}^{-1}$ and $K_0 \simeq 0.12 \text{ MPa.m}^{1/2}$ respectively. In this regime, the crack growth rate can be set by adjusting the external applied load for a measured crack length. The protocol is the following (see Prades et al. (2005) for details):

- a large load is applied to reach a velocity close to 10^{-8} m.s^{-1}
- the load is subsequently decreased to a value *inferior to* the prescribed velocity
- the load is increased again up to the value that corresponds to the prescribed velocity
- the force is then fixed to this value and the crack tip neighbourhood is probed by AFM at magnification ranging from $250 \times 250 \text{ nm}^2$ to $10 \times 10 \text{ }\mu\text{m}^2$.

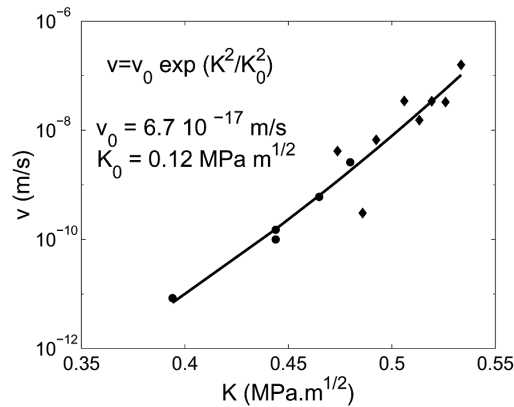
This procedure allows to have a ‘new’ crack tip with minimal corrosion ageing at the beginning of the observations.

3 Crack propagation within the process zone: evidence of nanoscale damage cavities

Our experimental setup allowed us to observe the crack progressing at the nanoscale, in real time, at the surface of the specimen. Figure 5(a)–(f) presents six successive frames in the vicinity of the crack tip, recorded during the five hours necessary for the crack front to cross the area of interest. For this particular sequence, the mean velocity of the crack growth was found to be $v = 4 \times 10^{-11} \text{ m.s}^{-1}$. One can clearly see on this sequence the growth of a depression ahead of the crack tip, of typically 100 nm in length and 25 nm in width. In other words, the crack front does not propagate regularly as commonly stated (Kelly et al., 1967; Lawn et al., 1980) but progresses through the growth and coalescence of cavities. This scenario is fully

consistent with what was observed both experimentally in aluminosilicate glasses under stress corrosion (Célarié et al., 2003a,b; Marlière et al., 2003) and numerically in dynamically breaking samples of amorphous silica (Kalia et al., 2003; Rountree, 2003; Rountree et al., 2002a; Van Brutzel, 1999; Van Brutzel et al., 2002).

Figure 4 Variation of the continuous crack tip velocity v (in $\text{m}\cdot\text{s}^{-1}$) as a function of the stress intensity factor (in $\text{MPa}\cdot\text{m}^{1/2}$). The black diamonds correspond to optical measurement and the black points correspond to AFM measurements



To ensure that the growing depression observed ahead the crack tip is actually a damage cavity, we analysed the *post-mortem* mismatch between the two crack lines using the Fracture Surface Topography Analysis (FRASTA) method (Célarié et al., 2003b; Kobayashi and Shockey, 1987; Miyamoto et al., 1990). In a ductile scenario, the growth of damage cavities is expected to induce irreversible plastic deformations that will leave visible prints on the developing fracture line. We have thus determined the crack lines after the crack has crossed the area of interest (white lines in Figure 5(f)) and reconstituted virtually the same material by placing the line on the right (line R) to the left of the line on the left (line L). Chronology of the cavity growth and crack progression is then obtained by gradually translating the line R to the right (Figure 5(a')–(f')). Let us note that the reconstructed cavity is found to be thinner than the real one. This is explained by the fact that the shape of the real cavity is given not only by the irreversible – plastic – part of the opening displacements at the free surface, but also by the reversible – elastic – one. This latter vanishes once the crack has crossed the area of interest and the stresses have relaxed, – and therefore cannot be taken into account in the reconstructed frames. Comparison between the real shapes of the main crack tip and cavities ahead (Figure 5(a')–(f')) and the reconstructed ones thus provides a method to evaluate the ratio between irreversible plastic deformations and reversible elastic ones.

4 Time evolution of damage cavities within the process zone

In order to investigate the precise kinematics of crack propagation within the process zone, we have determined the temporal evolution of point *A*, *B*, and *C* corresponding to the main crack front (CF), the forward front (FF) of the cavity and the backward

front (BF) of the cavity (see Prades et al. (2005)) for details on the procedure). The time evolution of the various tips is represented in Figure 6(a). Velocity of the three fronts was then calculated:

$$\begin{aligned} v^{CF} &\simeq 4 \times 10^{-12} \text{ m.s}^{-1} \\ v^{FF} &\simeq 1.1 \times 10^{-11} \text{ m.s}^{-1} \\ v^{BF} &\simeq 1.2 \times 10^{-11} \text{ m.s}^{-1}. \end{aligned} \quad (2)$$

All these velocities are significantly smaller than the mean crack tip velocity $\langle v \rangle = 4 \times 10^{-11} \text{ m.s}^{-1}$ as measured at the continuous scale. In other words, at these nanometric scales, the main crack front does not propagate regularly, but intermittently through the merging with the nanoscale cavities (Figure 6(b)). This has important consequences for the relevance of classical corrosion models at ultra-slow crack propagation: What sets the crack velocity at the continuum scale is not the rate at which bonds are broken at the crack tip as previously thought (Lawn, 1993; Wiederhorn, 1967), but rather the cavity size at coalescence and the frequency of coalescence events.

Figure 5 (a)–(f) Sequence of topographic AFM frames in the vicinity of the crack tip showing the propagation of a mode I crack along the x-axis. The scan size is $470 \times 135 \text{ nm}^2$ and the height range over 3 nm. The six frames were taken during the five hours necessary for the main crack to cross the area of interest. (a,b) apparition of a nanometric damage cavity ahead of the crack tip; (b–d) growth of the cavity prior to crack propagation; and (f,g) coalescence of the cavity with the main crack. The point *A*, *B* and *C* locate the position of the main crack tip (CF), the backward front (BF) and the forward front (FF) tips of the cavity respectively. (a')–(f') reconstructed frames using the FRASTA method (see text for details)

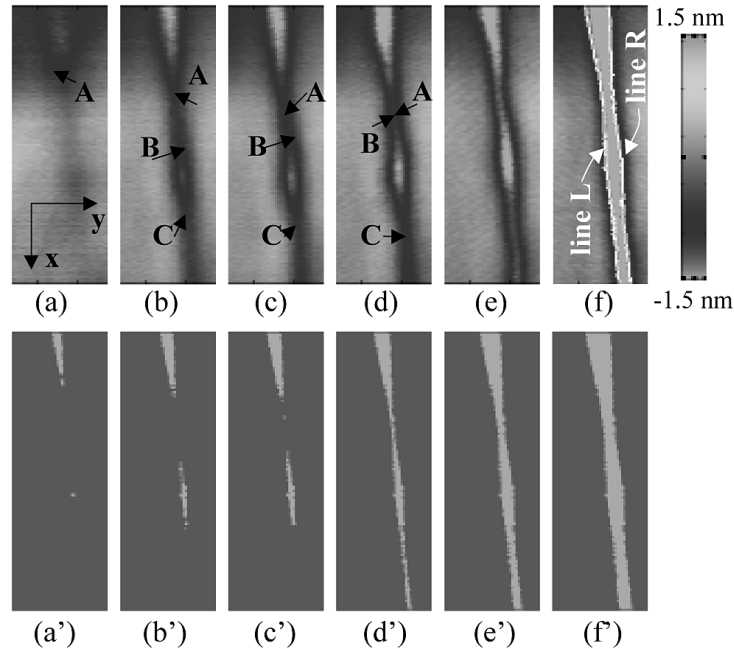
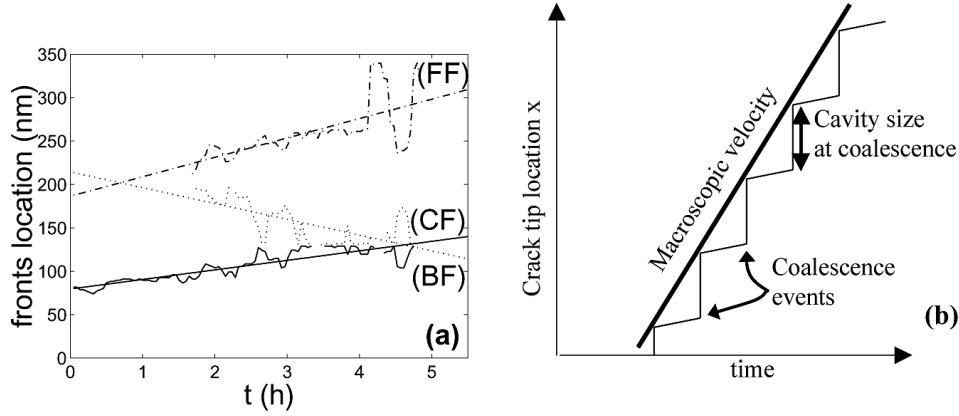


Figure 6 (a) Temporal evolution of the main crack front (CF) and the backward front (BF) of the cavity and the forward front (FF) of the cavity represented by point *A*, *B* and *C* on the frames of Figure 5(a)–(e) respectively. The velocities of these fronts are determined through linear fits: $v^{CF} \simeq 4 \times 10^{-12} \text{ m.s}^{-1}$, $v^{BF} \simeq 1.2 \times 10^{-11} \text{ m.s}^{-1}$ and $v^{FF} \simeq 1.1 \times 10^{-11} \text{ m.s}^{-1}$. The thicker line shows the velocity at the continuum scale: $\langle v \rangle \simeq 4 \times 10^{-11} \text{ m.s}^{-1}$. (b) Sketch of the crack tip propagation at scale of the process zone



5 Determination of the process zone size and its time evolution

The previous section was devoted to the way the crack tip propagates within the process zone at ultra-slow velocities. Let us now focus on the evolution of this process zone and determine its extension. Linear elastic theory predicts that the stress field is dominated by a square root singularity in the close vicinity of the crack tip (Irwin, 1958; Orowan, 1955). Calling σ the stress tensor and r the distance to the crack tip, one gets:

$$\sigma_{ij}(r) \propto \frac{1}{\sqrt{r}} \quad (3)$$

and, as long as the linear elastic stress strain relation held, one gets

$$\epsilon_{zz}(r) = \frac{\sigma_{zz} - \nu(\sigma_{xx} + \sigma_{yy})}{E} \quad (4)$$

where E , ν and ϵ refers to the Young modulus, the Poisson ratio and the strain tensor respectively. Near the crack tip, the out-of-plane displacement u_z at the free surface is thus expected to scale as:

$$u_z(r) \propto \frac{1}{\sqrt{r}}. \quad (5)$$

Measurement of u_z profiles have been performed on $1 \times 1 \mu\text{m}^2$ AFM topographical frames along the direction of crack propagation (see Célerié et al. (2003b) and Marlière et al. (2003) for details on the procedure). A typical u_z profile is shown in Figure 7. For r smaller than a given value R_c , u_z is found to depart from the $1/\sqrt{r}$

scaling predicted by linear elastic theory. This value R_c , around 200 nm sets the size of the process zone (see also Guilloteau et al. (1996) and Henaux and Creuzet (2000) for related discussion).

Figure 7 Measurement of the length of the process zone along the direction of crack propagation. (a) Typical $1 \times 1 \text{ m}^2$ AFM topographical frame of the vicinity of the crack tip. The black arrow and the r axis locates the crack tip and the line along which the out of plane displacement u_z are measured respectively. Variation of u_z as a function of the distance r from the crack tip. The axes are logarithmic. The straight line corresponds to the predictions of linear elasticity (Equation (5)). For $r \leq R_c$, u_z is observed to depart from the linear elastic predictions

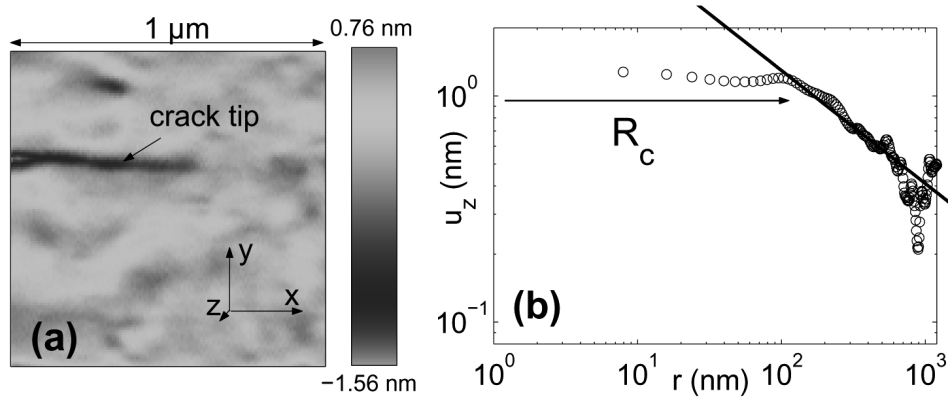
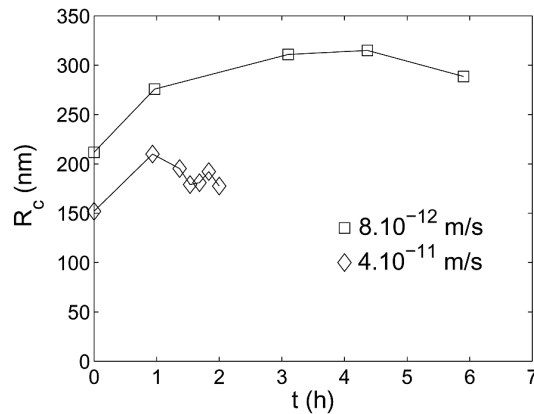


Figure 8 represents the time evolution of the process zone size R_c for two experiments performed at two crack growth velocities v , namely $v = 8 \times 10^{-12} \text{ m.s}^{-1}$ and $v = 4 \times 10^{-11} \text{ m.s}^{-1}$. It should be recalled here that our experimental procedure was chosen so that a ‘new’ crack tip with minimal corrosion ageing at the beginning of each series of observations performed at a given crack growth velocity (end of Section 2). One can clearly observe a transient regime where R_c increases with time before reaching its steady value. The observed duration of this transient regime – approximately one hour for $v = 8 \times 10^{-12} \text{ m.s}^{-1}$ – decreases with velocity, and becomes non-observable for v larger than $4 \times 10^{-11} \text{ m.s}^{-1}$. In other words, a partially cracked specimen of glass under stress corrosion does not develop instantaneously a process zone of constant size which would depend only on the value of the stress intensity factor at the crack tip.

The transient regime is conjectured to result from stress enhanced water diffusion within the process zone. In this scenario, water molecules travel over a typical distance $d \simeq 100 \text{ nm}$ in a typical time $\tau \simeq 1 \text{ h}$. The diffusion coefficient D is thus expected to be $D = d^2/\tau \simeq 10^{-14} \text{ cm}^2 \text{ s}^{-1}$. Let us note that this order of magnitude is much higher than the value commonly observed in silica glass in the absence of stress (around $10^{-19} \text{ m.s}^{-1}$), but broadly consistent with Tomozawa and Han’s measurements (1991) of water entry in silica glass under stress corrosion.

Figure 8 Evolution of the process zone as a function of time for a crack growth velocity $V = 8 \times 10^{-12} \text{ m.s}^{-1}$ and $V = 4 \times 10^{-11} \text{ m.s}^{-1}$



6 Influence of the chemical composition: Role of alkalis in a binary $\text{Na}_2\text{O}/\text{SiO}_2$ glass

Silicate glasses as fabricated by glass industries are far more complex than pure amorphous silica. In particular, non-glass-forming oxide, such as Na_2O that modify the primitive amorphous SiO_2 network (Zachariassen, 1932) are incorporated. In these glasses, alkalis such as Na are weakly bonded to the glass network (Greaves, 1985; Van Brutzel, 1999) and thus relatively mobile as compared to the other chemical components. This migration of sodium – enhanced by the stress field in the core region of the crack (Nghiem, 1999) – may alter significantly the mechanical properties of the glass.

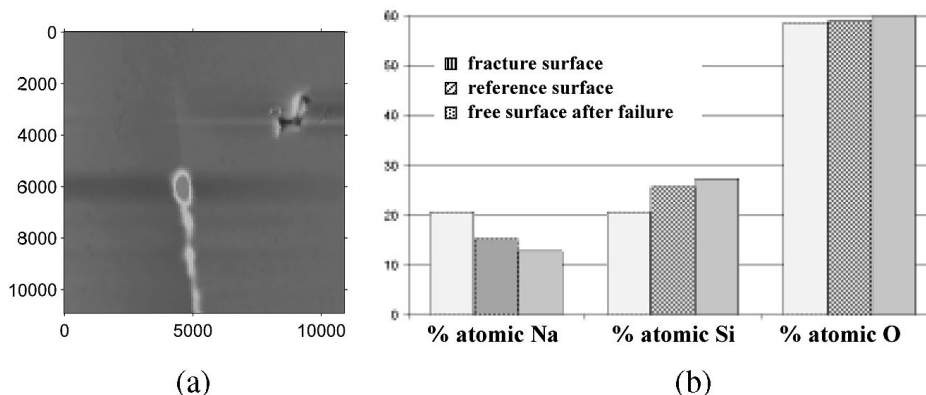
In order to evidence such sodium migration, we have observed slow crack propagation at the surface of binary 12.5% $\text{Na}_2\text{O}/87.5\%\text{SiO}_2$ and 25% $\text{Na}_2\text{O}/75\%\text{SiO}_2$ glasses under stress corrosion. A typical AFM topographical frame in the vicinity of the crack tip is depicted in Figure 9(a). Sub-micrometric bumps can clearly be distinguished within the process zone, along the two fracture lips.

To better understand the nature of these bumps, XPS analyses were performed with M-J Guittet on:

- the free surface of the sample before failure
- the free surface of the sample after failure
- the fracture surface after failure.

The results are reported in Figure 9(b). The fracture surface is found to be impoverished by Na while the free surface is enriched with Na. This strongly suggests that Na atoms migrate to the free surface via these bumps along the crack front during the failure. Let us add that very recent experiments performed by F. Célarié (2004) reveal that the evolution of these bumps is governed by the combinations of the stress field within the process zone, the relative humidity and the crack growth velocity.

Figure 9 (a) AFM frame of the vicinity of the crack front in a binary glass 25%Na₂O/75%SiO₂. Sub-micrometric bumps can be observed slightly behind the crack tip. (b) Comparisons of the atomic percentages in sodium, oxygen and silicon as measured by XPS on the free surface of the sample prior failure, the free surface after failure and the fracture surface after failure



7 Concluding discussion

Ultra-slow crack propagation was observed in real time at the nanoscale through AFM in both amorphous silica and binary Na₂O/SiO₂ glasses. The main results from our observations are:

- Within the process zone, the crack tip does not propagate regularly, but through the growth and coalescence of damage cavities.
- Velocity of the main crack tip and the cavity tips as measured at the damage zone scale is shown to be significantly smaller than the mean crack growth velocity as measured at the continuous scale. In other words, the crack growth is intermittent and dominated by the accelerating phases corresponding to the cavity coalescence with the main crack front.
- Damage in the vicinity of the crack tip induces a departure from stress field singularity predicted by LEFM. This provides a method to quantify the size of the process zone.
- By looking at the time evolution of the process zone size, we evidenced a transient regime where an increase of the process zone size with time is observed for the lowest velocity (around 10^{-11} m.s⁻¹). This time dependent regime is conjectured to be related to stress enhanced water diffusion within the process zone. This scenario is broadly consistent with measurements performed by Tomozawa and Han (1991) on water entry in silica glass under stress corrosion.
- AFM observations reveal that crack propagation in binary Na₂O/SiO₂ is accompanied by sub-micrometric exudations at the crack tip. Furthermore, XPS analysis shows that, during material failure, the vicinity of the crack tip gets impoverished with sodium while the free surface of the specimen gets enriched with sodium. These observations strongly suggest a stress-assisted migration of Na atoms out of the process zone during the glass failure.

Observations of damage cavities in amorphous silica under stress corrosion are consistent to what Célarié et al. (2003a,b) and Marlière et al. (2003) observed experimentally in aluminosilicate glasses under stress corrosion or numerically during dynamic failure of amorphous silica (Kalia et al., 2003; Rountree, 2003; Rountree et al., 2002a; Van Brutzel, 1999; Van Brutzel et al., 2002). This indicates that the existence of this nanoductile mode is inherent to the amorphous structure and does not depend on the precise glass composition. This leads us to think that the scenario observed in MD simulations of dynamic fractures (Kalia et al., 2003; Rountree, 2003; Rountree et al., 2002a; Van Brutzel, 1999; Van Brutzel et al., 2002) can be extended to the ultra-slow stress corrosion regime: The amorphous structure results in toughness fluctuations at the nanoscale that behave as stress concentrators and give birth to the observed damage cavities.

The intermittent progression of the crack tip evidenced at the scale of the process zone questioned the classical picture traditionally proposed to describe glass failure under stress corrosion: What set the crack growth velocity at the continuum scale is not the rate at which bonds are broken at the crack tip as previously thought (Lawn, 1993; Wiederhorn, 1967), but rather the cavity size at coalescence and the frequency of coalescence events. Understanding the relation between the glass composition and the cavity size then becomes of practical importance since the latter controls the crack growth velocity in sub-critical regime – and therefore the life expectancy over the long term. Work in this direction is currently in progress.

This mechanism of growth and coalescence of damage cavities ahead of the crack tip is very similar to what is observed classically – albeit at much larger length scales – in ductile metallic alloys where a crack progresses through the coalescence of damage cavities that nucleate in the vicinity of microstructural defects (Paun and Bouchaud, 2003). Similar cavitation mechanisms were also observed in nanophase materials (Kalia et al., 2003; Rountree, 2003; Rountree et al., 2002a,b), PMMA (Ravi-Chandar and Yang, 1997) and polymers (Lapique et al., 2002). We argue that such a mechanism is generic to crack propagation when it is observed on the scale of the material heterogeneity. This may explain why fracture surfaces are observed to be self-affine surfaces characterised by a universal roughness exponent, independent of both the precise nature of the materials and the failure mode (Bouchaud, 1997).

Let us finally add that, while the present investigation sheds light on the role played by material *spatial* fluctuations within the process zone, it does not tackle the aspect of *temporal* fluctuations. Interaction of a growing crack with the material micro-structure results in the release of acoustic waves (Bonamy and Ravi-Chandar, 2003, 2005; Ravi-Chandar and Knauss, 1984) that are not taken into account by LEFM. These waves appear to play a significant role in the energy dissipation properties of a propagating crack. Their understanding and characterisation then represent an interesting challenge for future investigation.

Acknowledgements

We acknowledge Marie-Jo Guittet for performing the XPS measurements and Thierry Bernard for his technical support. We are also indebted to Fabrice Célarié, Stephane Chapuliot, Rajiv Kalia, Christian Marlière, Krishnaswamy Ravi-Chandar,

Laurent Van Brutzel, and Sheldon Wiederhorn for enlightening discussions, and to the MATCO programme for its constant support. CLR is currently supported by a National Science Foundation Graduate Research Fellowship under grant no. 0401467.

References

- Bonamy, D. and Ravi-Chandar, K. (2003) 'Interaction of shear waves and propagating cracks', *Phys. Rev. Lett.*, Vol. 91, pp.235502/1–4.
- Bonamy, D. and Ravi-Chandar, K. (2005) 'Dynamic crack response to a localized shear pulse perturbation in brittle amorphous materials: on crack surface roughening', *Int. J. Fract.*, Vol. 134, pp.1–22.
- Bouchaud, E. (1997) 'Scaling properties of cracks', *J. Phys. Condens. Matt.*, Vol. 9, pp.4319–4344 (and references therein).
- Célarié, F. (2004) 'Dynamique de fissuration à basse vitesse des matériaux vitreux', PhD thesis, Université Montpellier II, France.
- Célarié, F., Prades, S., Bonamy, D., Dickele, A., Bouchaud, E., Guillot, C. and Marlière, C. (2003a) 'Surface fracture of glassy materials as detected by real-time atomic force microscopy (AFM) experiments', *Appl. Surf. Sci.*, Vol. 212, pp.92–96.
- Célarié, F., Prades, S., Bonamy, D., Ferrero, L., Bouchaud, E., Guillot, C. and Marlière, C. (2003b) 'Glass breaks like metal, but at the nanometer scale', *Phys. Rev. Lett.* Vol. 90, 075504/1–4.
- Ewalds, H.L. and Wanhill, R.J.H. (1985) *Fracture Mechanics*, London: Edward Arnold Limited.
- Freund, L.B. (1990) *Dynamic Fracture Mechanics*, Cambridge: Cambridge University Press.
- Greaves, G.N. (1985) 'EXAFS and the structure of glass', *J. Non.-Cryst. Solids*, Vol. 71, pp.203–217.
- Griffith, A.A. (1920) 'The phenomena of rupture and flows in solids', *Phil. Trans. Roy. Soc. London*, Vol. A221, pp.163–198.
- Guilloteau, E., Charrue, H. and Creuzet, F. (1996) 'The direct observation of the core region of a propagating fracture crack in glass', *Europhys. Lett.*, Vol. 34, pp.549–553.
- Henaux, S. and Creuzet, F. (2000) 'Crack tip morphology of slowly growing cracks in glass', *J. Am. Cer. Soc.*, Vol. 83, pp.415–417.
- Irwin, G.R. (1958) 'Fracture', in *Handbuch der Physik*, Berlin: Springer-Verlag, Vol. 6, p.551.
- Kalia, R.K., Nakano, A., Vashishta, P., Rountree, C.L., Van Brutzel, L. and Ogata, S. (2003) 'Multiresolution atomistic simulations of dynamic fracture in nanostructured ceramics and glasses', *Int. J. Fract.*, Vol. 121, pp.71–79.
- Kelly, A., Tyson, W.R. and Cottrell, A.H. (1967) 'Ductile and brittle crystals', *Philos. Mag.*, Vol. 15, p.567.
- Kobayashi, T. and Shockey, D.A. (1987) 'A fractographic investigation of thermal embrittlement in cast duplex stainless steel', *Metall. Trans. A*, Vol. 18A, pp.1941–1949.
- Lapique, F., Meakin, P., Feder, J. and Jossang, T. (2002) 'Self-affine fractal scaling in fracture in ethylene and propylene polymers surfaces generated and copolymers', *J. Appl. Pol. Sci.*, Vol. 86, pp.973–983.
- Lawn, B.R. (1993) *Fracture of Brittle Solids* (2nd edition), Cambridge: Cambridge University Press.
- Lawn, B.R., Hockey, B.J., and Wiederhorn, S.M. (1980) 'Atomically sharp cracks in brittle solids: an electron microscopy study', *J. Mater. Sci.*, Vol. 15, p.1207.
- Marlière, C., Prades, S., Célarié, F., Dalmas, D., Bonamy, D., Guillot, C. and Bouchaud, E. (2003) 'Crack fronts and damage in glass at the nanometre scale', *J. Phys.-Condens. Matt.*, Vol. 15, pp.2377–2386.

- Miyamoto, H., Kikuchi, M. and Kawazoe, T. (1990) 'A study on the ductile fracture of Al-alloys 7075 and 2017', *Int. J. of Fract.*, Vol. 42, p.389.
- Nghiem, B. (1999) 'Fracture du verre et hétérogénéités à l'échelle submicrométrique', PhD Thesis, Université Paris VI, France.
- Orowan, E. (1955) 'Energy criteria of fracture', *Energy Criteria of Fracture*, Vol. 34, p.157.
- Paun, F. and Bouchaud, E. (2003) 'Morphology of damage cavities in aluminium alloys', *Int. J. Fract.*, Vol. 121, pp.43–44.
- Pineau, A., Franois, D. and Zaoui, A. (1995) *Comportement mécanique des matériaux*, Paris: Hermès.
- Prades, S. (2004) 'Mécanismes de rupture du verre à l'échelle nanométrique', PhD thesis, Université Paris VI, France.
- Prades, S., Bonamy, D., Dalmas, D., Bouchaud, E. and Guillot, C. (2005) 'Nano-ductile crack propagation in glasses under stress corrosion: spatiotemporal evolution of damage in the vicinity of the crack tip', *Int. J. Sol. Struct.*, Vol. 42, pp.637–645.
- Ravi-Chandar, K. and Knauss, W.G. (1984) 'An experimental investigation into dynamic fracture – IV On the interaction of stress waves with propagating cracks', *Int. J. Fract.*, Vol. 26, pp.189–200.
- Ravi-Chandar, K. and Yang, B. (1997) 'On the role of microcracks in the dynamic fracture of brittle materials', *J. Mech. Phys. Solids*, Vol. 45, pp.535–563.
- Rice, J.M. (1968) 'A path independent integral and approximate analysis of strain concentration by notches and cracks', *J. Appl. Mech.* Vol. 35, pp.379–386.
- Rice, J.M. and Tracey, D.M. (1969) 'On ductile enlargement of voids in triaxial stress fields', *J. Mech. Phys. Sol.*, Vol. 17, pp.201–217.
- Rountree, C.L. (2003) 'Massively parallel molecular dynamics simulations of crack front dynamics and morphology in amorphous nanostructured silica', PhD Thesis, Louisiana State University, USA.
- Rountree, C.L., Kalia, R.K., Lidorikis, E., Nakano, A., Van Brutzel, L. and Vashishta, P. (2002a) 'Atomistic aspects of crack propagation in brittle materials: Multimillion atom molecular dynamics simulations', *Annu. Rev. Mat. Res.*, Vol. 32, pp.377–400.
- Rountree, C.L., Van Brutzel, L., Lidorikis, E., Nakano, A., Kalia, R.K. and Vashishta, P. (2002b) 'Atomistic simulations of nanoceramics', *Proceedings of CINTEC 2002, 10th International Ceramic Congress and 3rd Forum on New Materials*, P. Vincenzini (Ed), Florence, Italy, July 14–18, 2002.
- Tomozawa, M. and Han, W.H. (1991) 'Water entry into silica glass during slow crack growth', *J. Am. Cer. Soc.*, Vol. 74, pp.2573–2576.
- Van Brutzel, L. (1999) 'Contribution à l'étude des mécanismes de rupture dans les amorphes: Etude par dynamique moléculaire de la rupture de verre de silice', PhD thesis, Université Paris VI, France.
- Van Brutzel, L., Rountree, C.L., Kalia, R.K., Nakano, A. and Vashishta, P. (2002) 'Dynamic fracture mechanisms in nanostructured and amorphous silica glasses: million-atom molecular dynamics simulations', *Materials Research Society Symposium Proceedings*, 13.9.1–V.3.9.6, p.703.
- Wiederhorn, S.M. (1967) 'Influence of water vapor on crack propagation in soda-lime glass', *J. Am. Cer. Soc.*, Vol. 50, pp.407–414.
- Wiederhorn, S.M. and Bolz, L.H. (1970) 'Stress corrosion and static fatigue of glass', *J. Am. Cer. Soc.*, Vol. 53, pp.543–548.
- Zachariasen, W.H. (1932) 'The atomic arrangement in glass', *J. Am. Cer. Soc.*, Vol. 54, p.3841.